

Modulation of inflammatory processes by thermal stimulating and RPE regenerative laser therapies in age related macular degeneration mouse models

Elisabeth Richert^b, Claus von der Burchard^b, Alexa Klettner^b, Philipp Arnold^c, Ralph Lucius^c, Ralf Brinkmann^{d,e}, Johann Roider^b, Jan Tode^{a,b,*}

^a Hannover Medical School, Department of Ophthalmology, Hannover, Germany

^b Christian-Albrechts-University of Kiel, Department of Ophthalmology, University Medical Center, Kiel, Germany

^c Christian-Albrechts-University of Kiel, Institute of Anatomy, Kiel, Germany

^d Medical Laser Center Lübeck, Lübeck, Germany

^e Institute for Biomedical Optics, University of Lübeck, Lübeck, Germany

ARTICLE INFO

Keywords:

Selective Retina Therapy (SRT)
Thermal Stimulation of the Retina (TSR)
Age-related Macular Degeneration (AMD)
Inflammation
Laser Therapies

ABSTRACT

Purpose: Inflammatory processes play a major role within the multifactorial pathogenesis of age-related macular degeneration (AMD). Neuroretina sparing laser therapies, thermal stimulation of the retina (TSR) and selective retina therapy (SRT), are known to reduce AMD-like pathology in vitro and in vivo. We investigated the effect of TSR and SRT on inflammatory processes in AMD mouse models.

Methods: One randomized eye of 8 months old apolipoprotein (Apo)E and 9 months old nuclear factor (erythroid-derived 2) -like 2 (NRF2) knock out mice were treated by TSR (10 ms, 532 nm, 50 μm^2 spot size, mean 4.5 W, ~200 spots) or SRT (~1.4 μs pulses, 532 nm, 50 μm spot size, 100 Hz over 300 ms, mean 2.5 μJ per pulse, ~200 spots). Fellow eyes, untreated knock out mice and wild-type BL/6J mice acted as controls. All mice were examined funduscopically and by optical coherence tomography (OCT) at the day of laser treatment. Mice were euthanized and enucleated either 1 day or 7 days after laser treatment and examined by gene expression analysis of 84 inflammatory genes.

Results: The inflammatory gene expression profile of both knock out models compared to healthy BL/6J mice suggests a regulation of pro- and anti-inflammatory processes especially concerning T-cell activity and immune cell recruitment. TSR resulted in downregulation of several pro-inflammatory cell-mediators both in ApoE -/- and NRF2-/- mice compared to treatment naïve litter mates one day after treatment. In contrast, SRT induced pro-inflammatory cell-mediators connected with necrosis one day after treatment as expected following laser-induced selective RPE cell death. Seven days after laser treatment, both findings were reversed.

Conclusions: Both TSR and SRT influence inflammatory processes in AMD mouse models. However, they act conversely. TSR leads to anti-inflammatory processes shortly after laser therapy and induces immune-cell recruitment one week after treatment. SRT leads to a quick inflammatory response to laser induced RPE necrotic processes. One week after SRT inflammation is inhibited. It remains unclear, if and to what extent this might play a role in a therapeutic or preventive approach of both laser modalities on AMD pathology.

1. Introduction

Age related macular degeneration (AMD) is the most common cause for legal blindness in the industrialized world [1,2]. Following the Beckmann classification [3] of AMD, it can be divided into an early, an intermediate and two late forms. The early form is characterized by metabolic deposits in and around retinal pigment epithelium (RPE)

[4–6] macroscopically called drusen. Large drusen combined with signs of RPE malfunction clinically presenting as pigmentary abnormalities, like pigment clumping [7], define intermediate AMD. Late-stage AMD is either characterized by chorioretinal (geographic) atrophy (non-exudative (dry) AMD), or by the presence of choroidal neovascularization (CNV) and called neovascular AMD (nAMD). Both late forms of AMD lead to vision loss and eventually to legal blindness. The pathogenesis of

* Corresponding author at: Hannover Medical School, Department of Ophthalmology, Carl-Neuberg-Str. 1, 30625 Hannover, Germany.
E-mail address: tode.jan@mh-hannover.de (J. Tode).

<https://doi.org/10.1016/j.cyttox.2020.100031>

Received 30 April 2020; Received in revised form 10 June 2020; Accepted 12 June 2020

Available online 20 June 2020

2590-1532/ © 2020 The Author(s). Published by Elsevier Ltd. This is an open access article under the CC BY-NC-ND license (<http://creativecommons.org/licenses/by-nc-nd/4.0/>).

CNV is known to be driven by highly increased intraocular secretion of vascular endothelial growth factor (VEGF). Hence, intravitreal anti-VEGF agents are standard of care for nAMD [8]. Despite the success of anti-VEGF treatment, patients may still become blind due to central fibrosis and atrophy [9] in the long-term course of disease. The pathogenesis of early and intermediate stages of AMD as well as geographic atrophy is not entirely understood and has many environmental, behavioral and genetic influences [10,11]. Numerous pathological processes continuously build up and interdigitate on their way from asymptomatic early AMD to sight-threatening advanced AMD. Impaired lipid metabolism [4] as well as oxidative stress [12,13] are considered as initial steps in AMD development. Lipids within the Choroid/Bruch's membrane (BrM)/retinal pigment epithelium (RPE)/Photoreceptor-Complex [14,15] mostly originate from photoreceptor outer segment metabolism [16,17] and lipoprotein metabolism of RPE. The role of lipid and lipoprotein levels in blood is believed to be less important [18]. Accumulated lipids, undegradable lipoproteins and other substances in and around BrM are biochemically altered and oxidized [19–21], especially in the macula region where oxidative stress is known to be pronounced [22,23]. Oxidized lipids are known to induce the innate immunity, microglial activity and RPE cell death [24–27]. This may lead to the activation of pattern recognition receptors, like toll-like receptors [28]. The following formation of the inflammasome [29–31] activates immune cells and microglia to clear Choroid/BrM/RPE from various intra- and extracellular pathogens. These processes are not pathologic themselves. They are needed to keep a homeostatic environment. In AMD, they are pathologically over-active. An over-active inflammasome, driven by oxidized lipids and perhaps a genetically induced over-activity of complement [32], leads to an increased IL-1 β and IL18 [25,33] expression as well as the induction of other pro-inflammatory cytokines, such as IL-6 and TNF- α . This pro-inflammatory environment activates immune cells and in combination with peroxidized lipids may evoke AMD progression with cell death leading to atrophy [34–36] or CNV formation [37,38].

A therapeutic strategy for the treatment of early and intermediate AMD should save inflammation homeostasis at choroid/BrM/RPE and therefore keep physiological metabolic processes. Moreover, it should inhibit the over-expression of pro-inflammatory mediators to prevent disease progression. Novel strategies aiming at a specific part of the immune system, like lapaizumab (Roche) targeting complement factor D, have not shown to be effective [39]. This might be due to the selectivity of the target which would only affect a small part of the multifactorial disease. Dietary anti-oxidants to reduce oxidative stress at the choroid/BrM/RPE level and thereby inflammation driven disease progression, like examined by the AREDS study, only showed little progression-preventive effect for a certain group of patients with advanced AMD [40]. Currently, there is no pathogenesis driven treatment neither for early or intermediate AMD nor for geographic atrophy, although many therapeutic ideas have been proposed.

Neuroretina sparing laser modalities like thermal stimulation of the retina (TSR) and RPE-regenerative selective retina therapy (SRT) both induce a multitude of processes with possible therapeutic implications for early and intermediate AMD. In previous studies we could show that both laser modalities induce the expression of active metalloproteinases in vitro and reduce the pathologically thickened BrM in murine AMD models [41–44]. The morphological structure of RPE cells is revitalized and renewed. Furthermore, proangiogenic VEGF is reduced while anti-angiogenic PEDF induced by SRT and TSR [41–43]. Hence, both laser modalities act at multiple levels, however they have not entirely been investigated. So far, we do not know their effect on inflammatory processes. Both an induction or an inhibition of inflammatory processes by the laser treatments are feasible. As inflammatory processes are important for the development of AMD, this is an important aspect to study to address the potential beneficial and harmful effects of neuroretina sparing laser treatment.

In this study, we investigated SRT and TSR induced regulation of

pro- and anti-inflammatory mediators in two murine AMD models. The above described interacting pathomechanisms of lipid accumulation and oxidative stress are well resembled by the AMD mouse models chosen. The apolipoprotein(Apo)E knock out mouse model is known to accumulate lipids in BrM [45–47] followed by inflammatory processes. The nuclear factor (erythroid-derived 2) -like 2 (NRF2) knock out mouse model lacks an important anti-oxidative transcription factor resulting in increased oxidative stress in RPE [48] with extra cellular matrix modifications, inflammatory processes and altered angiogenesis [49].

2. Materials and methods

2.1. AMD mouse models

Both knock out AMD mouse models have been described in detail before [42,45,49]. We chose 8 months old ApoE -/- knock out mice, for we have shown before, that this genotype expresses the wanted AMD-like phenotype at that age. Likewise, we chose 9 months old NRF2 -/- knock out mice, for we have shown the AMD-like phenotype at that age before [42,43]. Wild-type C57BL/6J mice were age-matched. Both strains (ApoE -/- and NRF2 -/-) as well as the C57BL6/J control mice were purchased from the Jackson Laboratories (Bar Harbour, ME, USA) and housed and bred at the local university animal care unit. The homozygous genotype was confirmed by PCR from tail clips. Also, Crumbs homologue1 (CRB1) retinal degeneration (rd)8 mutation was genotyped, for it is known that CRB1^{rd8} interferes with the AMD phenotype of NRF2-/- mice [50]. Mice carrying the mutation were excluded from breeding. Mice were kept on a regular 12 h night and day cycle and fed standard murine diet and water ad libitum. All animal experiments were conducted in accordance with EU directive 2010/63/EU for animal experiments. They were approved by the animal ethics and welfare committee (approval number: V 242–7224.121–12 (61–5/14)) located at the ministry of energy transition, agriculture, environment and rural areas in Schleswig-Holstein according to German federal and European law. Animal experiments adhered to the ARVO statement for the use of animals in ophthalmic and vision research.

2.2. Animal maintenance and anesthesia during experiments

All examinations and laser treatment were conducted under general anesthesia. Deep anesthesia was induced by an intraperitoneal injection of a mixture of 0.05 mg/kg body weight Fentanyl (Braun, Melsungen, Germany), 5.0 mg/kg body weight Midazolam (Hameln Pharma, Hameln, Germany) and 0.5 mg/kg bodyweight Medetomidin (CP-Pharma, Bergdorf, Germany).

The animal was then placed on a rigid examination platform and body temperature was maintained within normal parameters using a heating mat. Pupils were dilated by 0.025 mg/ml Phenylephrine and 0.05 g/ml Tropicamide (UKSH Pharmacy, Kiel, Germany). Eyes were covered with a protective moisturizing gel (2% Methylcellulosis Methocel®, Puchheim, Germany). After examinations, the anesthesia was antagonized by a mixture of 1.2 mg/kg bodyweight Naloxon (Braun), 0.5 mg/kg bodyweight Flumazenil (Inresa GmbH, Freiburg, Germany) and 2.5 mg/kg bodyweight Atipamezol (Orion Pharma, Espoo, Finland). Anesthesia was uneventful in all mice. Animal well-being was evaluated by a standard score sheet and was uneventful in all included mice. After the final examination animals were euthanized by cervical dislocation at the day of enucleation under deep anesthesia.

2.3. Examinations

All examinations were conducted under general anesthesia. All mice were examined by funduscopy using a contact fundus camera (MICRON III, phoenix research labs, Pleasanton, CA, USA). The integrity of the retina was assessed, the number of drusen-like retinal spots (DRS) was

counted, RPE atrophy evaluated, and CNV noted.

Optical coherence tomography (OCT) (small animal OCT, thorlabs, Lübeck, Germany) was applied via contact optics to evaluate the retinal structure, confirm retinal integrity after laser treatment, and to confirm CNV. After laser treatment, it was used to investigate anatomical integrity of retinal layers.

All examinations were repeated at the day of enucleation, thus 1 day or 1 week after laser treatment. Untreated controls also were examined twice, at inclusion and at enucleation day.

2.4. Laser treatment

For both SRT and TSR a frequency doubled Neodym-Vanadate (Nd:VO₄) experimental laser (Carl Zeiss Meditec AG, Jena, Germany) with a wavelength of 532 nm was used. The light was coupled to an optical multimode fiber of square cross section with a 70 × 70 μm core profile. The laser light was applied via contact laser-injector (Phoenix) attached to the Micron III camera. The aiming beam laser was controlled visually via Micron III live fundus imaging. Spot size was determined by the size of the laser fiber and laser injector, fixed to 50 μm² and could not be changed.

For TSR duration of irradiation was fixed to 10 ms of continuous constant power. For SRT duration of irradiation was fixed to 300 ms creating 30 pulses per spot at a repetition rate of 100 Hz, each with a pulse-duration of ~1.4 μs. Similar to our previous work [42,43], the intended effect was titrated visually by decreasing energy at the peripheral retina from a clearly visible white burn at higher energy to a barely visible spot at lower energy. The barely but instantly visible spot was classified as threshold of definite retinal burn/RPE destruction with visible neuroretinal involvement. Power/energy was reduced by 70% to ensure a temperature increase that does not lead to thermal damage to RPE nor neuroretina for TSR and to ensure selective RPE lesion without damage to neuroretina respectively. The invisible 50 μm TSR/SRT laser spots were distributed uniformly across the retina at 1 spot interspot spacing to an optic disc centered approx. 50° field of view. No laser spot was aimed at vasculature or the optic disc. Laser treatments were carried out at inclusion day.

2.5. Inflammatory gene arrays

RT² profiler PCR array (Qiagen®, Frederick, Maryland, USA; Mouse Inflammatory Response & Autoimmunity; PAMM-077Z) was used to determine regulation of inflammation related mediators of AMD mouse model mice compared to wildtype mice and TSR or SRT treated eyes in comparison with untreated fellow control eyes. The anterior segment including cornea, conjunctiva, iris, lens, ciliary body of enucleated eyes was removed, and eyes were immediately frozen in liquid nitrogen for later use. For RNA isolation, eyes were incubated with 20 μl dilution buffer and 0.5 μl RNA release for 7 min. at room temperature and 3 min. at 98 °C. Tissues were centrifuged for 2 min. at 13,000 rpm and supernatants were placed in a new 1.5 ml collection tube.

Eyes were homogenized using 1 ml TRI Reagent® (Sigma-Aldrich) and 5 ceramic beads (Precellys Bulk Beads 1,4 mm Zirconium oxide beads) and the tissue homogenizer Precellys® (5000 rpm, 2 × 20 sec). Afterwards total RNA from posterior eye segment was isolated using TRI Reagent® according to the manufacturer's instructions.

Isolated RNA was converted to cDNA using the RT2 First Strand Kit (Qiagen). The mixture was aliquoted (25 μl) to each well of the same RT2 Profiler PCR Array plate (96-well plate) containing the pre-dispensed gene-specific primer sets. PCR was performed using a 7500 Fast Real Time cycler (Applied Biosystems).

Qiagens online Web analysis tool (Gene globe) was used to calculate the fold change by determining the ratio of mRNA levels to control values using the Δ threshold cycle (Ct) method ($2^{-\Delta\Delta C_t}$). All data were normalized to the housekeeping genes of PAMM007Z panel. PCR conditions used: hold for 10 min at 95 °C, followed by 40 cycles of 15 s at

95 °C and 60 s at 60 °C.

2.6. Statistics

Fold changes in gene expression for pairwise comparison using the $\Delta\Delta C_t$ method was calculated through Qiagen® Web analysis tool and p-values were provided, at a confidence interval of 95% and a type-1 error of 5%. For comparison of the knock-out genotypes ApoE^{-/-} (8 months old) and NRF2^{-/-} (9 months old) with wild-type C57BL/6J mice (8 months and 9 months old respectively), groups of 6 randomized eyes each were chosen.

For comparison of TSR or SRT treated to untreated eyes, one randomized eye of ApoE^{-/-} or NRF2^{-/-} was treated by TSR or SRT. One day or one week after treatment these eyes were compared to entirely untreated age-matched randomized control eyes of the same genotypes in groups of 6 eyes each.

3. Results

3.1. In-vivo imaging

Mice were examined and lasered at the age of 8 months for ApoE^{-/-} and 9 months for NRF2^{-/-}. All mice showed signs of AMD, like drusen-like retinal spots (DRS), RPE pigmentation irregularities and mottling (see Fig. 1). CNV or geographic atrophy, as marker for late AMD, was not seen in any mouse. AMD disease grading, as described before in Richert et al. 2020 [50] (1 = physiological retina, 2 = 1–14 DRS, 3 = 15–100 DRS, 4 = > 100 DRS, 5 = any number of DRS plus signs of late AMD), revealed a mean of grade 2.3 ± 0.6 in NRF2^{-/-} and 1.8 ± 0.5 in ApoE^{-/-} mice. These values did not differ statistically significant before compared to one week after laser treatment. There were no signs of neuroretinal damage as determined by fundus examination or OCT after laser irradiation. One day after SRT, pigment irregularities correlating to the applied laser spots were noted in 3 out of 12 eyes.

3.2. PCR-array for the expression level of inflammatory cell mediators

The expression level of inflammatory cell mediators was examined by RT² profiler PCR array in wild-type BL/6J mice and compared to untreated control ApoE^{-/-} and NRF2^{-/-} mice.

In ApoE^{-/-} mice an upregulation of early response Fos as well as pro-inflammatory pyrogen and lymphocyte mitogen interleukin (IL)-1 receptor, complement and tumor-necrosis-factor (Tnf) α were seen. T-cell associated IL-17 and IL-22 and chemokine CCL-22 were downregulated. In NRF2^{-/-} mice, an upregulation of early response Fos and IL-6 as master regulator of immune response was found (see Fig. 1).

The comparison of untreated control knock-out mice with laser treated mice on day 1 and day 7 after either TSR or SRT revealed different responses, depending on time after treatment and laser modality applied. Independently of the genotype, TSR led to a downregulation of pro-inflammatory and pro-immune cell-attractive cell mediators 1 day after treatment. 7 days after treatment monocyte and lymphocyte attractive mediators and some pro-inflammatory cytokines were upregulated. SRT, on the other hand, led to an increased RNA-expression of pro-inflammatory and pro-immune cell-attractive cell mediators as well as complement and cell detritus and waste recognizing toll-like receptor system, one day after treatment. Conversely, seven days after SRT, pro-inflammatory mediators, complement and toll-like system members were downregulated (see Fig. 2).

In detail (see Table1), TSR inhibited inflammatory processes and immune cell attraction one day after treatment in both ApoE^{-/-} and NRF2^{-/-}-mice. Chemokine systems attracting monocytes, lymphocytes and neutrophils, namely chemokine ligands (Ccl1,20,22,24; Cxcl9,11) and Chemokine receptors (Ccr 4,7; Cxcr1), pro-inflammatory interleukins (IL-5,9,17,23), macrophage attractant Interferon(Ifn)- γ , pro-

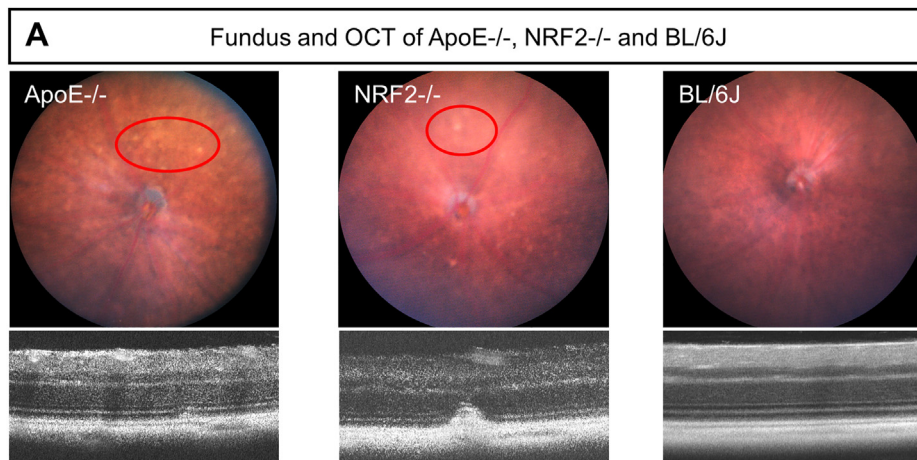


Fig. 1. Wild-type BL/6J, ApoE^{-/-} and NRF2^{-/-} mouse model. **A:** Representative fundus (above) and Optical Coherence Tomography (OCT, below) images of 8 months old ApoE^{-/-} (left), 9 months old NRF2^{-/-} (middle) and 8 months old BL/6J (right) mice. Note the drusen-like retinal spots and their OCT-correlate. **B:** Table of the inflammatory mediator up- (white) and down-regulation (grey). Note that in untreated litter mate ApoE^{-/-} mice there was a higher number of altered inflammatory cell mediators than in untreated litter mate NRF2^{-/-} mice. **C:** Table of the inflammatory mediator up- (white) and down-regulation (grey). Note that in untreated litter mate NRF2^{-/-} mice there was a lower number of altered inflammatory cell mediators than in ApoE^{-/-}.

B Gene Expression in ApoE^{-/-} Mice Compared to BL/6J

cell mediator	function	expression	p-value
Fos	cell growth, angiogenesis	2.4 fold	0.01
IL1-R	MP/recruitment, inflammasome	2.1 fold	<0.001
TNF α	pro-inflammatory regulator	2.9 fold	0.02
C3	complement	2.1 fold	0.05
IL-22, IL-17a	immune response and T-cell induction	- 3.4 fold - 6.2 fold	0.004 0.02
Ccl22	Homeostasis of immunesystem	-6.5 fold	0.02
Fas	apoptosis	-3.4 fold	0.03

C Gene Expression in NRF2^{-/-} Mice Compared to BL/6J

cell mediator	function	expression	p-value
Fos	cell growth, angiogenesis	3.38 fold	0.049
IL-6	master regulator of immune response	2.33 fold	0.048

inflammatory lymphotoxins (Lt)a and b, leukocyte pro-adhesive kinyogen (Kng)1, first response nitrous oxide system (Nos) and T-cell stimulating tumor necrosis factor stimulating factor (Tnfsf)14 were all downregulated one day after TSR in ApoE^{-/-} mice. Only follicular T-cell stimulating B-cell lymphoma factor (Bcl)6 and Toll-like-receptor superfamily (Tirap) were upregulated. In NRF2^{-/-} mice, pro-inflammasome IL-1 and pro-inflammatory IL-6 stimulating CCAAT/enhancer binding protein β (Cebpb), pro-inflammatory IL-5, leukocyte pro-adhesive selectin (Sele) and cell-detritus recognizing Toll-like receptors (Tlr4,7,9) were down-regulated.

Seven days after TSR, the picture was different. For both ApoE^{-/-} and NRF2^{-/-} mice, an upregulation of monocyte/lymphocyte attractant chemokines and immune cell binding proteins was seen, without pro-inflammatory cell mediators. In ApoE^{-/-} mice Chemokines Ccl2,7,12

Ccr3, Cxcl1,5 and Sele were upregulated. Chaperone heat shock protein 90 was downregulated. In NRF2^{-/-} mice Chemokines Ccl2 and Ccl5 were upregulated, Ccr20 was downregulated. Cluster of differentiation (Cd)40 ligand, specific for activated T cells was upregulated. T-helper (h) cell specific IL-9 and leukocyte adhesion promoting integrin subunit β 2 (Itgb2) were also upregulated. IL-6 receptor and IL-22 were down-regulated.

The inflammatory processes after SRT treatment looked entirely different. In ApoE^{-/-} mice one day after SRT, complement system factors C3, C4b and C3 receptor as well as complement stimulating C-reactive protein were upregulated. Chemokines Ccl5, 17, Cxcr4, antigen presenting CD40, macrophage differentiating colony-stimulating factor (Csf)1 and epithelial to mesenchymal transition (EMT) inducing Fos were upregulated. Induction of pro-inflammatory cytokine IL-1

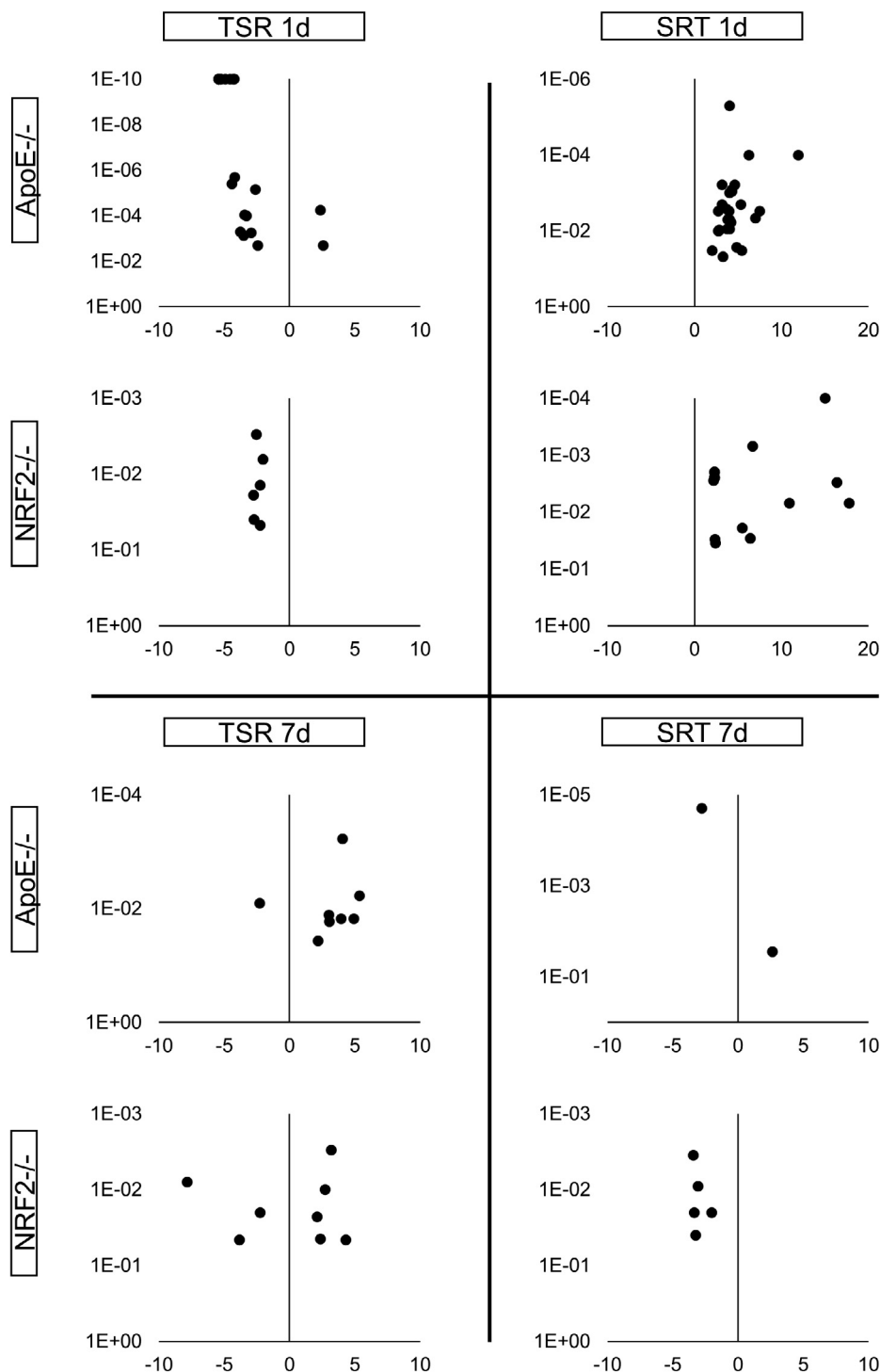


Fig. 2. Distribution of pro-inflammatory mediators in laser treated eyes compared to untreated controls. X-axis displays the x-fold expression of inflammatory cell mediators; Y-axis provides the p-values. Only statistically significant values are displayed. Each dot represents one mediator. Minus values represent a down-regulation, plus values an up-regulation. It can clearly be seen that TSR inhibits and SRT induces inflammatory processes one day after treatment. Seven days after treatment these processes are different and partly reversed. Single analysis with values provided are given in Table 1.

receptors and IL-6 receptor, interleukin inducing Bcl6 and pro-inflammatory cytokine enhancing nuclear factor kappa-light-chain-enhancer of activated B cells (Nfkb)1, as well as Nfkb-inducing receptor-interacting serine/threonine-protein kinase (Ripk)2 was found. Leucocyte adhesive Itgb2, inflammation cell signaling promoting myeloid differentiation primary response (Myd)88, cell stress responsive nuclear factor 3, group C (Nr3c)1 and HSP-90 were all up-regulated. Furthermore, cell detritus recognizing toll-like receptor

system, namely Tlr2, 4, 9, Tirap, lymphotoxin (Ly)96, toll-interacting protein (Tollip), was upregulated. The only anti-inflammatory cell mediator upregulated was IL-10 receptor β (IL10rb).

In NRF2-/- mice one day after SRT, a similar picture was seen. Leukocyte attractant chemokines and their receptors, namely Ccl1, 2, 7, 8, 12, 20, 24, Ccr4, Cxcl2, 3, Cxcr2 were upregulated. Activated T-cell ligand CD40lg and cell mobility enhancing kininogen Kng1 were upregulated. Pro-inflammatory cytokines Ifn- γ , autoimmunity cytokine IL-

Table 1

Single Values of Examined Inflammatory Cell Mediators. Column 1 shows the name of the protein examined. For each genotype, x-fold expression in the treated eyes (TSR or SRT respectively) compared with untreated eyes and their p-values are given. Only statistically significant values are displayed.

prot	ApoE								NRF2								
	TSR1d		TSR7d		SRT1d		SRT7d		TSR1d		TSR7d		SRT1d		SRT7d		
	fold	p	fold	p	fold	p	fold	p	fold	p	fold	p	fold	p	fold	p	
Bcl6	2.37	0.000057			7.46	0.003											
C3					4	0.009											
C3ar1					3.18	0.002											
C4b					5.41	0.033											
Ccl1	-5.41	1E-10											2.27	0.002			
Ccl12			3.04	0.017			2.63	0.028					5.5	0.019			
Ccl17					4.04	0.005											
Ccl2			4.06	0.0006							2.36	0.045	6.42	0.029			
Ccl20	-4.4	0.000004									-7.86	0.008	2.27	0.002			
Ccl22	-4.3	1E-10															
Ccl24	-5.41	1E-10											2.27	0.002			
Ccl5					3.28	0.048					2.73	0.01					
Ccl7			3.95	0.015									17.74	0.007			
Ccl8													6.69	0.0007			
Ccr3			3.01	0.013													
Ccr4	-5.28	1E-10											2.27	0.0025			
Ccr7	-3.78	0.0005															
Cd40					3.79	0.005											
Cd40lg	-5.41	1E-10									4.32	0.046	2.27	0.0025			
Cebpb									-2.73	0.04							
CRP					4.84	0.027											
Csf1					4.29	0.0008											
Cxcl1			5.36	0.006													
Cxcl11	-4.23	1E-10															
Cxcl2													15.03	0.0001			
Cxcl3													16.34	0.003			
Cxcl5			4.91	0.015													
Cxcl9	-3.5	0.000757											2.27	0.0025			
Cxcr1	-4.2	0.000002															
Cxcr2													2.27	0.0025			
Cxcr4					2.82	0.0095											
Fos					7.01	0.0046	-2.79	0.00002									
Ifng	-5.41	1E-10											2.27	0.0025			
Il10	-4.92	1E-10											2.27	0.0025			
Il10rb					3.16	0.0006											
Il17a	-5.41	1E-10											2.27	0.0025			
Il1b																	-2.01 0.02
Il1r1					4.02	0.000005											
Il1rap					3.64	0.0026											
Il1rn													10.87	0.007			
Il22											-2.27	0.02					
Il23a	-3.31	0.0001											2.18	0.0028			
Il23r	-4.56	1E-10											2.34	0.03			
Il5	-2.42	0.002							-2.77	0.019							
Il6ra					3.74	0.009					-3.83	0.046					
Il9	-5.41	1E-10									3.21	0.003					
Itgb2					2.76	0.01					2.12	0.023					
Kng1	-5.41	1E-10											2.27	0.0025			
Lta	-5.26	1E-10											2.27	0.0025			
Ltb	-2.94	0.00057											2.27	0.0025			
Ly96					2.02	0.033											
Myd88					6.25	0.0001											
Nfkb1					4.6	0.0006											
Nos2	-2.6	0.000007															
Nr3c1					4.29	0.0009											
Ripk2					2.74	0.003											-3.26 0.04
Sele			2.18	0.037							-2.27	0.014					
Tirap	2.59	0.002			11.9	0.0001											-3.35 0.02
Tlr1													2.42	0.035			
Tlr2					3.96	0.003											
Tlr4					2.75	0.01					-2.05	0.0064					
Tlr7											-2.27	0.047					
Tlr9					4.2	0.006					-2.53	0.003					
Tnfsf14	-3.44	0.00009															
Tollip					4.02	0.001											
Hsp90			-2.29	0.008	5.32	0.002											

17a, pyogenic IL-1receptor, IL-1 family inducing IL-23a and its receptor IL-23r, pro-inflammatory lymphotoxins (Lt)a and b were upregulated. Toll-like receptor 1 RNA-expression was increased. The only anti-inflammatory cytokine increased was IL-10.

However, 7 days after SRT, the the expression patterns were different. In ApoE^{-/-} mice, monocyte attractant Ccl12 was upregulated, EMT-inducing Fos downregulated. In NRF2^{-/-} mice, Complement factor C4b, pyrogenic IL-1b, stress-response signal Nr3c1, toll-like receptor system Tirap and pro-inflammatory cytokine inducing Bcl6 were all downregulated.

4. Discussion

The intention of this study was to investigate the influence of neuroretina sparing SRT and neuroretina and RPE sparing TSR on inflammatory processes of eyes showing AMD-like alterations of the choroid/BrM/RPE-complex. The examined expression of 84 genes provides a good picture of genes relate to leukocyte attraction and adhesion molecules (chemokines, kininogen, lymphocyte adhesion molecules), antigen presentation and recognition of cell waste and detritus (toll-like-receptor system), innate immune system (complement), pro- and anti-inflammatory cytokines (interleukins, TNF) and the acquired immune system (T-cell stimulation and differentiation).

Both included AMD mouse models are known to undergo pathological alterations that resemble an AMD phenotype with drusen and or RPE mottling. We show here that both models also display alterations of inflammatory processes. These processes are more pronounced in ApoE^{-/-} mice compared to NRF2^{-/-} which show only little alterations. In ApoE^{-/-} mice cell-growth and pro-angiogenic Fos, pro-inflamasome IL-1 receptor, immune-regulator TNF α and complement factor 3 are upregulated, whereas pro-inflammatory IL-22 and IL-17a, chemokine Ccl22 and Fas were downregulated. In NRF2^{-/-} only Fos and inflammation master regulator IL-6 were upregulated. Besides restoration of choroid/BrM/RPE-complex anatomy, as shown before [42,43], the goal of TSR and SRT is to reduce pro-inflammatory processes, known to play an important role in AMD, and likewise to induce inflammation homeostasis. We show here that the influence of TSR and SRT laser treatment on inflammation differs depending on the kind of laser treatment. The two mouse models exhibited comparable reactions to the respective laser treatments, although these models resemble different pathogenetic aspects of AMD (lipid metabolism alterations in ApoE^{-/-} and oxidative stress in NRF2^{-/-}). Our data therefore strongly indicate that the immune-processes following laser-treatment do not depend on the pathological pathway of the respective mouse model but depend on the treatment modality.

TSR is a laser modality that transiently increases temperature within RPE without destroying these cells or adjacent photoreceptors and choroid [42]. One day after treatment, TSR results in a reduction of immunological action in retinal tissue by downregulation of genes involved in immune-cell attraction, differentiation and adhesion, pro-inflammatory cytokines, and antigen presenting and cell detritus recognizing receptors. One week after TSR, however immune-cell attraction molecules are upregulated, possibly to enable recognition and removal of cell debris.

SRT, on the other hand, leads to an increased immunological answer immediately after treatment. SRT is a pulsed laser modality that intentionally disrupts RPE cells. Unaffected neighboring RPE cells proliferate, migrate and thereby regenerate the RPE monolayer afterwards [41]. Therefore, necrosis is expected and of course accompanied by inflammation. One day after SRT leukocyte attraction and adhesion, pro-inflammatory cell-mediators, antigen presentation and cell detritus/death and waste recognition, first response and acute phase protein RNA as well as complement are upregulated. The upregulation of anti-inflammatory IL-10 could suggest active phagocytosis of necrosis danger-signals. These parts of the inflammatory response are known in necrosis and therefore are a direct consequence of RPE disruption. Toll-

like-receptors recognize parts of the destroyed cells and transmit their signal through NF κ b, Ifn- γ , IL-1 [51] and others, all of which are up-regulated one day after SRT. This answer leads to a quick cleaning of the RPE environment from cell detritus and possibly other harmful substances like oxidized lipids that have pathologically accumulated in AMD. One week after SRT, immune response is downregulated in parts and homeostasis likely rebuilt. The restoration of inflammation homeostasis would have a positive effect on the otherwise pro-inflammatory environment seen in AMD.

TSR initially blocks parts of the ocular immune system. This could be beneficial in terms of AMD treatment. It is unknown why an increase in temperature within RPE leads to such a response. It might be a tissue protective answer. It might lead to a downregulation of pre-inflamed tissue surrounding RPE, such as neuroretinal tissue in AMD. Activated microglia might thereby return to their watchful resting state. SRT on the other hand initially leads to increased inflammatory processes induced by cell necrosis. One could argue that this will lead to increased AMD pathology. However, a renewal of RPE might also lead to removal of pathological RPE that induces inflammation and thereby lead to a beneficial process in terms of AMD. Morphologically we could show before that both AMD-mouse models return to physiological properties one month after SRT showing reducing AMD-like morphology.

We can clearly show that TSR and SRT differ entirely in their immunological response which needs to be considered when using these therapies in patients. Further investigations need to be conducted to fully elucidate the effects and their consequences. Moreover, different AMD disease stages might react differently to either laser treatment. The consequences of the treatment may be related to the immunological state of the respective AMD stage. We know that both TSR and SRT similarly alter morphological pathology of BrM and RPE in AMD mouse models restoring a more physiological phenotype. It is not clear, if the investigated laser effects on inflammation influence AMD pathology, since SRT and TSR strongly differ in their inflammatory reaction.

As a limitation of this study, the reliance on PCR-array, which only examines the RNA level, but not the protein level or actual cell involvement, can be questioned. However, gene arrays are a highly accepted method to evaluate inflammatory responses [52–54] and because of the larger number of genes examined, the array gives an excellent overview on the tissue reaction. Nevertheless, protein expression and histological examination of retinal tissue investigating cells of the immune system should be examined in further studies.

Another limitation is the limited amount of time points we have examined. The immune response is likely to change between the two chosen time points and later time points. However, the use of animals and the necessity to reduce the experimental burden and number of animals sacrificed limit the number of time points that can be justified [55]. Easier to use cell or organ culture models are inadequate to study the inflammatory response to these laser modalities, since systemic immune cells are missing in these models. That explains also, why nearly no inflammatory response to SRT in an organ culture model could be shown in previously [56]. A general limitation considering the translation into the human situation is the use of mouse models, as the murine systems lack the anatomical region of a macula. They can only reflect AMD pathology in parts. Therefore, more research is needed, especially clinical trials, to investigate a possible therapeutic effect of TSR and SRT on AMD. Still, the use of mice can model aspects of AMD [57] and our previous work [41–43] and work of other groups [58] have shown promising data and give a strong indication that these therapies should be further tested.

5. Conclusion

TSR and SRT act contrarily on inflammatory processes. TSR initially inhibits an immune response and later expresses genes indicating immune cell recruitment. SRT initially induces inflammation linked to

necrosis and later expresses genes that restore inflammation homeostasis. TSR and SRT influence inflammatory processes that might be related to AMD, thereby providing evidence to act as therapeutic option for AMD. Both laser modalities warrant further examination.

CRediT authorship contribution statement

Elisabeth Richert: Conceptualization, Methodology, Software, Validation, Formal analysis, Resources, Supervision. **Claus Burchard:** Writing - review & editing. **Alexa Klettner:** Methodology, Resources. **Philipp Arnold:** Methodology, Resources, Writing - review & editing. **Ralph Lucius:** Resources, Writing - review & editing. **Ralf Brinkmann:** Resources, Writing - review & editing. **Johann Roeder:** Resources, Writing - review & editing. **Jan Tode:** Conceptualization, Methodology, Software, Validation, Formal analysis, Resources, Supervision, Writing - review & editing.

Declaration of Competing Interest

The authors declare that they have no known competing financial interests or personal relationships that could have appeared to influence the work reported in this paper.

Acknowledgments

Funding

Research presented here was funded by Helmut Ecker Stiftung.

We thank Gaby Steinkamp (MTA von Lucius), Mandy Götz for their excellent technical assistance.

Declaration of Competing Interest

There is no conflict of interest.

Animal Experiments Ethical Approval

All experiments were approved by the local ethics committee situated at the ministry of energy, agriculture, environment, nature and digitalization in Schleswig-Holstein, Germany acting on German federal and European law (V242-7224.121-12(61-5/14)).

References

- W.F. Schrader, Age-related macular degeneration: a socioeconomic time bomb in our aging society, *Ophthalmol. Z. Dtsch. Ophthalmol. Ges.* 103 (2006) 742–748.
- R. Klein, B.E. Klein, K.L. Linton, Prevalence of age-related maculopathy. The Beaver Dam Eye Study, *Ophthalmology* 99 (1992) 933–943.
- F.L. Ferris, et al., Clinical classification of age-related macular degeneration, *Ophthalmology* 120 (2013) 844–851.
- C.A. Curcio, M. Johnson, M. Rudolf, J.-D. Huang, The oil spill in ageing Bruch membrane, *Br. J. Ophthalmol.* 95 (2011) 1638–1645.
- C.A. Curcio, C.L. Millican, Basal linear deposit and large drusen are specific for early age-related maculopathy, *Arch. Ophthalmol. Chic. Ill* 1960 (117) (1999) 329–339.
- C.A. Curcio, C.L. Millican, T. Bailey, H.S. Kruth, Accumulation of cholesterol with age in human Bruch's membrane, *Invest. Ophthalmol. Vis. Sci.* 42 (2001) 265–274.
- A. Okubo, et al., The relationships of age changes in retinal pigment epithelium and Bruch's membrane, *Invest. Ophthalmol. Vis. Sci.* 40 (1999) 443–449.
- CATT Research Group et al. Ranibizumab and bevacizumab for neovascular age-related macular degeneration. *N. Engl. J. Med.* 364 (2011) 1897–1908.
- J.E. Grunwald, et al., Growth of geographic atrophy in the comparison of age-related macular degeneration treatments trials, *Ophthalmology* 122 (2015) 809–816.
- L.G. Fritsche, et al., A large genome-wide association study of age-related macular degeneration highlights contributions of rare and common variants, *Nat. Genet.* 48 (2016) 134–143.
- M.M. DeAngelis, et al., Genetics of age-related macular degeneration (AMD), *Hum. Mol. Genet.* 26 (2017) R45–R50.
- J.G. Hollyfield, et al., Oxidative damage-induced inflammation initiates age-related macular degeneration, *Nat. Med.* 14 (2008) 194–198.
- Z. Wu, T.W. Lauer, A. Sick, S.F. Hackett, P.A. Campochiaro, Oxidative stress modulates complement factor H expression in retinal pigmented epithelial cells by acetylation of FOXO3, *J. Biol. Chem.* 282 (2007) 22414–22425.
- J.P. Sarks, S.H. Sarks, M.C. Killingsworth, Evolution of geographic atrophy of the retinal pigment epithelium, *Eye Lond. Engl.* 2 (Pt 5) (1988) 552–577.
- C.A. Curcio, C.L. Millican, Basal linear deposit and large drusen are specific for early age-related maculopathy, *Arch. Ophthalmol. Chic. Ill* 1960 (117) (1999) 329–339.
- S.M. Zekavat, J. Lu, C. Maugeais, N.A. Mazer, An in silico model of retinal cholesterol dynamics (RCD model): insights into the pathophysiology of dry AMD, *J. Lipid Res.* 58 (2017) 1325–1337.
- F. Storti, et al., Regulated efflux of photoreceptor outer segment-derived cholesterol by human RPE cells, *Exp. Eye Res.* 165 (2017) 65–77.
- Y. Wang, et al., The association between the lipids levels in blood and risk of age-related macular degeneration, *Nutrients* 8 (2016).
- R.F. Spaide, W.C. Ho-Spaide, R.W. Browne, D. Armstrong, Characterization of peroxidized lipids in Bruch's membrane, *Retina Phila. Pa* 19 (1999) 141–147.
- E.F. Moreira, I.M. Larrayoz, J.W. Lee, I.R. Rodríguez, 7-Ketocholesterol is present in lipid deposits in the primate retina: potential implication in the induction of VEGF and CNV formation, *Invest. Ophthalmol. Vis. Sci.* 50 (2009) 523–532.
- J.R. Beattie, et al., Multiplex analysis of age-related protein and lipid modifications in human Bruch's membrane, *FASEB J. Off. Publ. Fed. Am. Soc. Exp. Biol.* 24 (2010) 4816–4824.
- T. Zhang, et al., Human macular Müller cells rely more on serine biosynthesis to combat oxidative stress than those from the periphery, *eLife* 8 (2019).
- P. Gouras, L. Ivrt, M. Neuringer, T. Nagasaki, Mitochondrial elongation in the macular RPE of aging monkeys, evidence of metabolic stress, *Graefes Arch. Clin. Exp. Ophthalmol. Albrecht Von Graefes Arch. Klin. Exp. Ophthalmol.* 254 (2016) 1221–1227.
- K. Kaarniranta, et al., Fatty acids and oxidized lipoproteins contribute to autophagy and innate immunity responses upon the degeneration of retinal pigment epithelium and development of age-related macular degeneration, *Biochimie* (2018), <https://doi.org/10.1016/j.biochi.2018.07.010>.
- A. Kauppinen, J.J. Paterno, J. Blasiak, A. Salminen, K. Kaarniranta, Inflammation and its role in age-related macular degeneration, *Cell. Mol. Life Sci.* 73 (2016) 1765–1786.
- A. Klettner, et al., Cellular and molecular mechanisms of age-related macular degeneration: from impaired autophagy to neovascularization, *Int. J. Biochem. Cell Biol.* 45 (2013) 1457–1467.
- Q. Xu, S. Cao, S. Rajapakse, J.A. Matsubara, Understanding AMD by analogy: systematic review of lipid-related common pathogenic mechanisms in AMD, AD, AS and GN, *Lipids Health Dis.* 17 (2018) 3.
- T. Kawai, S. Akira, The role of pattern-recognition receptors in innate immunity: update on Toll-like receptors, *Nat. Immunol.* 11 (2010) 373–384.
- V. Tarallo, et al., DICER1 loss and Alu RNA induce age-related macular degeneration via the NLRP3 inflammasome and MyD88, *Cell* 149 (2012) 847–859.
- S.L. Doyle, et al., NLRP3 has a protective role in age-related macular degeneration through the induction of IL-18 by drusen components, *Nat. Med.* 18 (2012) 791–798.
- A. Kauppinen, et al., Oxidative stress activates NLRP3 inflammasomes in ARPE-19 cells—implications for age-related macular degeneration (AMD), *Immunol. Lett.* 147 (2012) 29–33.
- D.D.G. Despriet, et al., Complement factor H polymorphism, complement activators, and risk of age-related macular degeneration, *JAMA* 296 (2006) 301–309.
- R. Iijima, et al., Interleukin-18 induces retinal pigment epithelium degeneration in mice, *Invest. Ophthalmol. Vis. Sci.* 55 (2014) 6673–6678.
- D. Ricklin, G. Hajishengallis, K. Yang, J.D. Lambris, Complement: a key system for immune surveillance and homeostasis, *Nat. Immunol.* 11 (2010) 785–797.
- J. Ambati, J.P. Atkinson, B.D. Gelfand, Immunology of age-related macular degeneration, *Nat. Rev. Immunol.* 13 (2013) 438–451.
- D.S. Boyer, U. Schmidt-Erfurth, M. van Lookeren Campagne, E.C. Henry, C. Brittain, The pathophysiology of geographic atrophy secondary to age-related macular degeneration and the complement pathway as a therapeutic target, *Retina Phila. Pa* 37 (2017) 819–835.
- K. Tamai, et al., Lipid hydroperoxide stimulates subretinal choroidal neovascularization in the rabbit, *Exp. Eye Res.* 74 (2002) 301–308.
- B. Baba, et al., A rat model for choroidal neovascularization using subretinal lipid hydroperoxide injection, *Am. J. Pathol.* 176 (2010) 3085–3097.
- F.G. Holz, et al., Efficacy and safety of lomalizumab for geographic atrophy due to age-related macular degeneration: chroma and spectri phase 3 randomized clinical trials, *JAMA Ophthalmol.* 136 (2018) 666–677.
- Age-Related Eye Disease Study Research Group, A randomized, placebo-controlled, clinical trial of high-dose supplementation with vitamins C and E and beta carotene for age-related cataract and vision loss: AREDS report no. 9, *Arch. Ophthalmol. Chic. Ill* 1960 (119) (2001) 1439–1452.
- E. Richert, et al., Release of different cell mediators during retinal pigment epithelium regeneration following selective retina therapy, *Invest. Ophthalmol. Vis. Sci.* 59 (2018) 1323–1331.
- J. Tode, et al., Thermal stimulation of the retina reduces Bruch's membrane thickness in age related macular degeneration mouse models, *Transl. Vis. Sci. Technol.* 7 (2018) 2.
- J. Tode, et al., Selective retina therapy reduces Bruch's membrane thickness and retinal pigment epithelium pathology in age-related macular degeneration mouse models, *Transl. Vis. Sci. Technol.* 8 (2019) 11.
- E. Richert, et al., Response of RPE-choroid explants to thermal stimulation therapy of the retinal pigment epithelium (TS-R), *Invest. Ophthalmol. Vis. Sci.* 57 (2016) 4442.
- S. Dithmar, C.A. Curcio, N.A. Le, S. Brown, H.E. Grossniklaus, Ultrastructural changes in Bruch's membrane of apolipoprotein E-deficient mice, *Invest. Ophthalmol. Vis. Sci.* 41 (2000) 2035–2042.
- P. Yang, et al., Complement-mediated regulation of apolipoprotein E in cultured

- human RPE cells, *Invest. Ophthalmol. Vis. Sci.* 58 (2017) 3073–3085.
- [47] C.A. Curcio, Soft drusen in age-related macular degeneration: biology and targeting via the oil spill strategies, *Invest. Ophthalmol. Vis. Sci.* 59 (2018) AMD160–AMD181.
- [48] K.T. Vu, J.D. Hulleman, An inducible form of Nrf2 confers enhanced protection against acute oxidative stresses in RPE cells, *Exp. Eye Res.* 164 (2017) 31–36.
- [49] Z. Zhao, et al., Age-related retinopathy in NRF2-deficient mice, *PLoS One* 6 (2011) e19456.
- [50] E. Richert, A. Klettner, C. von der Burchard, J. Roeder, J. Tode, CRB1rd8 mutation influences the age-related macular degeneration phenotype of NRF2 knockout mice and favors choroidal neovascularization, *Adv. Med. Sci.* 65 (2020) 71–77.
- [51] K.L. Rock, H. Kono, The inflammatory response to cell death, *Annu. Rev. Pathol.* 3 (2008) 99–126.
- [52] D. Xia, A. Sanders, M. Shah, A. Bickerstaff, C. Orosz, Real-time polymerase chain reaction analysis reveals an evolution of cytokine mRNA production in allograft acceptor mice, *Transplantation* 72 (2001) 907–914.
- [53] C.A. Baker, L. Manuelidis, Unique inflammatory RNA profiles of microglia in Creutzfeldt-Jakob disease, *Proc. Natl. Acad. Sci. U. S. A.* 100 (2003) 675–679.
- [54] T. Naserpour Farivar, M. Nassiri-Asl, P. Johari, R. Najafipour, F. Hajiali, The effects of kainic acid-induced seizure on gene expression of brain neurotransmitter receptors in mice using RT2 PCR array, *Basic Clin. Neurosci.* 7 (2016) 291–298.
- [55] B. Rusche, The 3Rs and animal welfare - conflict or the way forward? *ALTEX* 20 (2003) 63–76.
- [56] E. Richert, et al., Effect of selective retina therapy (SRT) on the inflammatory microenvironment of the subretinal space, *Klin. Monatsbl. Augenheilkd.* 237 (2020) 192–201.
- [57] M.E. Pennesi, M. Neuringer, R.J. Courtney, Animal models of age related macular degeneration, *Mol. Aspects Med.* 33 (2012) 487–509.
- [58] A.I. Jobling, et al., Nanosecond laser therapy reverses pathologic and molecular changes in age-related macular degeneration without retinal damage, *FASEB J.* 29 (2015) 696–710.